

Late Vendian Complexes in the Structure of Metamorphic Basement of the Fore Range Zone, Greater Caucasus

V. A. Kamzolkin^{a, *}, A. V. Latyshev^{a, b}, Yu. P. Vidyapin^a, M. L. Somin^a,
A. I. Smul'skaya^a, and S. D. Ivanov^a

^a*Schmidt Institute of Physics of the Earth, Russian Academy of Sciences, Moscow, 123242 Russia*

^b*Department of Geology, Moscow State University, Moscow, 119991 Russia*

**e-mail: vkamzolkin@gmail.com*

Received September 22, 2017

Abstract—The paper presents new data on the composition, age, and relationships (with host and overlying deposits) of intrusive rocks in the basement of the Fore Range zone (Greater Caucasus), in the Malaya Laba River Basin. The evolutionary features of intrusive units located within the Blyb metamorphic complex are described. It is shown for the first time that the lower levels of this complex are, in a structural sense, outcrops of the Late Vendian basement. The basement is composed of the Balkan Formation and a massif of quartz metadiorites that intrudes it; for the rocks of this massif, ages ranging from 549 ± 7.4 to 574.1 ± 6.7 Ma are obtained for three U–Pb datings by the SHRIMP-II method. The Herzyinan magmatic event is represented by a group of granodiorite intrusions penetrating the Blyb complex on a series of faults extending along its boundary with the Main Range zone. The obtained estimate for the U–Pb age of one of the intrusions (319 ± 3.8 Ma) corresponds to the end of the Serpukhovian stage of the Early Carboniferous.

Keywords: Greater Caucasus, Fore Range zone, Main Range zone, structural geology, Blyb metamorphic complex, Late Vendian basement, geochronology, U–Pb dating, anisotropy of magnetic susceptibility

DOI: 10.1134/S0016852118030020

INTRODUCTION

The Fore Range zone possesses a complex structure and contains the longest geological record in the Greater Caucasus. In this respect, studies of its structure and evolution are fundamental for understanding the tectonics and geodynamics of the entire Greater Caucasus. At the base of the section of the Fore Range zone, crystalline schists and gneisses of the Blyb metamorphic complex occur; they are believed to be a parautochthonous complex or a pseudobasement [33]. Above it, a packet of tectonic thrust sheets (nappes) occurs, including, in particular, Paleozoic (Silurian–Lower Carboniferous) complexes: the Kizilkol (Urup) volcanic–sedimentary, Andryuki–Tokhana ophiolitic, and Atsgara metamorphic complexes [33]. The thrust sheets are overlain by deposits of a neoautochthonous molasse complex, which in turn range from Late Viséan to Early Triassic in age.

Studies of the age and structure of the base of the zone section, represented by the Blyb metamorphic complex, and analysis of its relationships with the overlying Urup complex make up the background for modern ideas about the Paleozoic evolution of the Fore Range, Greater Caucasus, and stirred certain debates. For example, the relationships between the Blyb and Urup complexes were considered as infra-

structural and suprastructural [1, 11, 12] or basement and sedimentary cover [10, 13], but in both cases the age of Blyb complex rocks was believed to be Lower Paleozoic. According to other viewpoints, Silurian–Devonian arc complexes could have been thrust upon the Precambrian basement [2, 3] or tectonically coupled with partially coeval rocks of the Blyb complex [6, 7].

High-pressure and high-temperature metamorphism were revealed for the Blyb complex [4], as well as a Middle Paleozoic age [33], which was younger with respect to that of the Urup complex, which underwent alteration under greenschist low-pressure facies.

The obtained age and structural data for the Blyb complex can supplement the research results on its associated intrusive bodies, in particular, the Balkan granitoid massif that occupies the central position in the structure of the crystalline basement of the Fore Range zone [4, 33] (Fig. 1). The Balkan massif is located in the interfluvium of the Bolshaya and Malaya Laba rivers; it is a large granitoid pluton of complex structure. According to the A.A. Samokhin's model [11], this massif intruded crystalline gneisses and schists of the Blyb metamorphic complex to form a dome. However, there are no signs of dome-shaped structures in the vicinity of the Balkan massif (Fig. 2), whereas flakelike

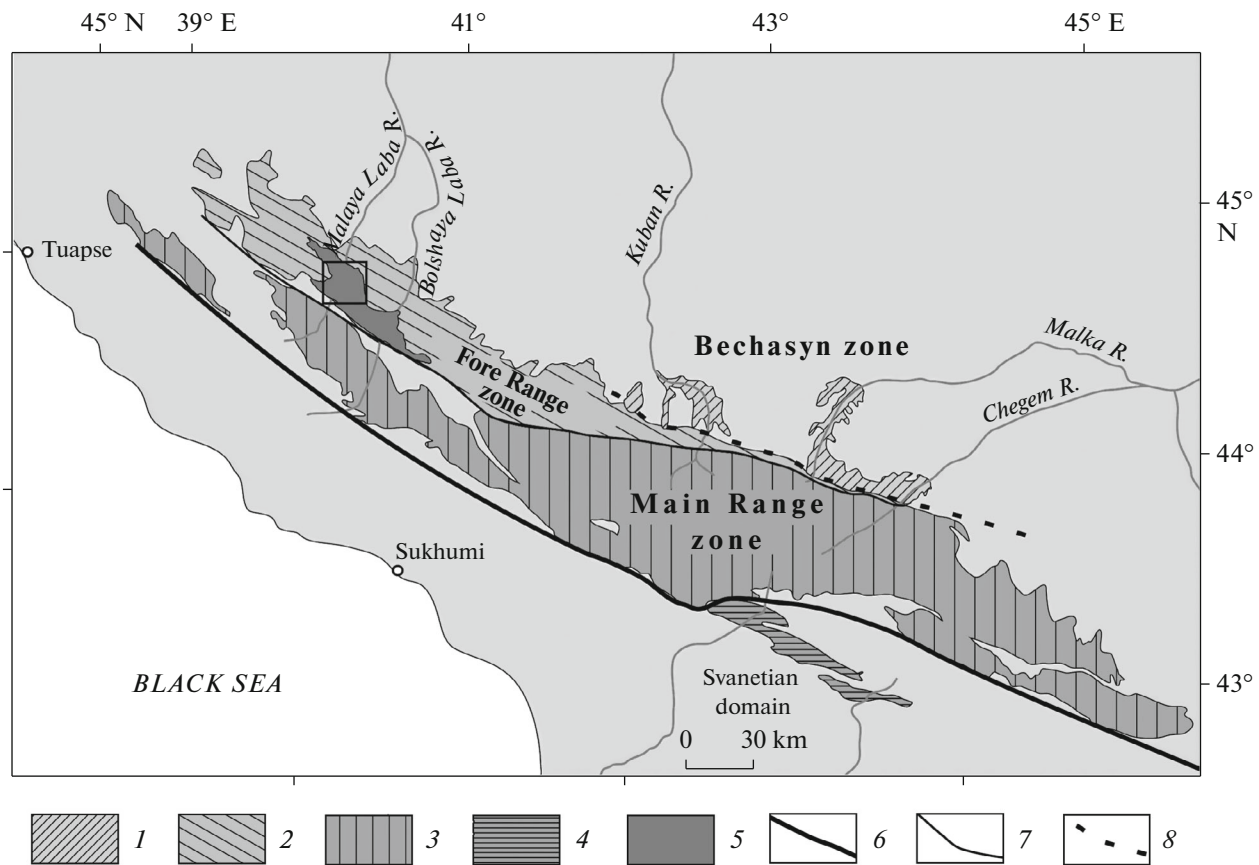


Fig. 1. Scheme of tectonic zoning of pre-Jurassic basement in Greater Caucasus region. Rectangle denotes study area. (1) Bechasyn zone; (2) Fore Range zone; (3) Main Range zone; (4) outcrops of Dizi Series rocks; (5) Blyb metamorphic complex; (6) Main Caucasian Fault; (7) Pshekish-Tyrnyauz zone; (8) boundary between Fore Range and Bechasyn zones.

structures are predominant [4]. Our comprehensive studies allowed us to obtain new data on the composition and evolution of intrusive bodies in the Malaya Laba River area, and also the data on their age and relationships with the host and overlying rocks.

We performed petrographic analysis of the rock composition of the Balkan massif and the Southern intrusive body and their metamorphic evolution. We carried out U–Pb dating of rock samples from the mentioned intrusive objects. Also, we studied the anisotropy of magnetic susceptibility of granitoids from the Balkan massif and Southern intrusive body and their host metamorphic complexes to obtain new data on the local stress fields when the granitoids of the Blyb metamorphic complex formed.

The aim of this work was to study intrusive bodies of the Blyb metamorphic complex, the conditions and time of their intrusion, and features of their metamorphic evolution.

BALKAN MASSIF

Rocks of the Balkan massif (Fig. 2) are characterized by the following mineral composition: 25% are

composed of amphibole, biotite, chlorite, and muscovite; 50%, plagioclase; and 25%, quartz. The color index of rock is M25, which is quite high.

These rocks are characteristic of irregularly-spotted structure with quartz lenses, feldspar clusters, and amphibole–biotite–chlorite–muscovite aggregates. The last mentioned aggregates are sometimes cut by kink zones with fine mica flakes transversely arranged in them. The texture of the initial rock was supposedly hypidiomorphic (granitoid), with the predominance of tabular plagioclase (of up to 5 mm in size); plagioclase is the only mineral that can be reliably referred to igneous. Quartz is concentrated in monomineral lenses of up to 5 mm in size with plagioclase relics inside and is a secondary mineral, whereas igneous quartz grains typical of granitoids are not seen in interstitials between feldspars. Superimposed quartz probably dominates in the rock. The other minerals are also of secondary character and form superimposed units. Chlorite–mica aggregates form a texture of chaotic flakes, probably in pseudomorphs on igneous mafic mineral. Within the bands and slabs of kink zones, flaked minerals are arranged perpendicularly to the boundaries of bands, forming a comblike texture. Gra-

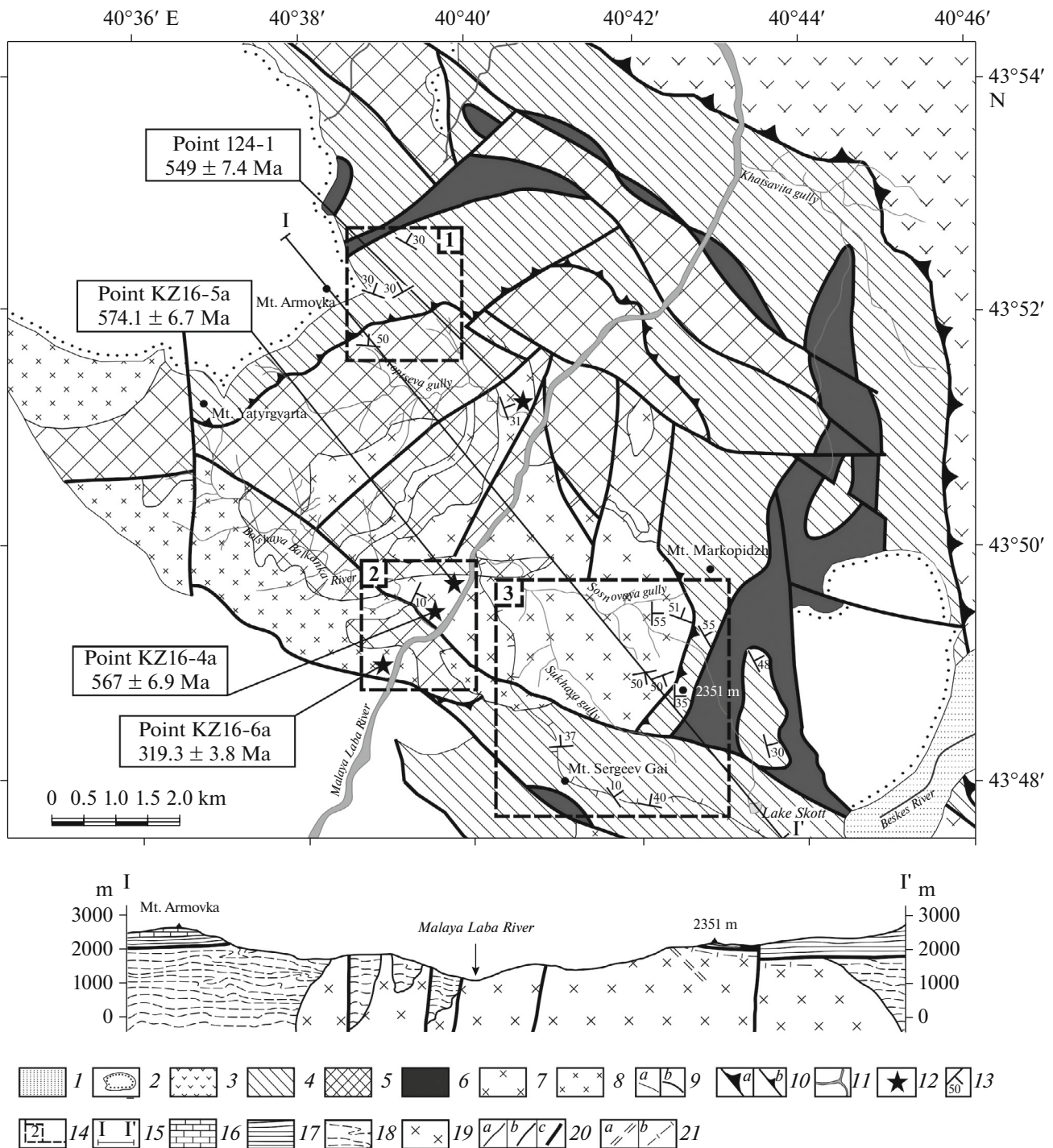


Fig. 2. Scheme of tectonic structure of Blyb metamorphic complex in Malaya Laba River Basin and schematic geological cross section (with data from [5]). (1) Cenozoic and Quaternary rocks; (2) Jurassic sedimentary rocks; (3) rocks of Urup volcanogenic–sedimentary complex; (4) Armovka Formation metamorphic rocks; (5) Balkan Formation; (6) hyperbasites; (7) Balkan metadiorite massif; (8) granodiorites of Southern intrusive body; (9) geological boundaries: (a) stratigraphic, (b) tectonic; (10) boundaries of nappes: (a) Urup, (b) Armovka; (11) rivers; (12) sampling points for geochronological studies (with sample numbers and respective ages); (13) orientations of mesoscopic foliation; (14) areas of detailed studies; (15) section line; (16–22) arbitrary notes in schematic geological cross section: (16) Lower–Middle Triassic limestones; (17) gneisses of Armovka nappe; (18) gneisses and amphibolites of Balkan Formation; (19) quartz metadiorites of Balkan massif; (20) geological boundaries: (a) stratigraphic, (b) intrusive, (c) tectonic; (21) foliation: (a) gneissic structure in quartz metadiorites, (b) occurrence of blastomylonite member.

noblastic textures of secondary quartz lenses have superimposed corrosion of plagioclase relics. Another form of superimposed units is undeveloped skeleton poikiloblasts of light bluish amphibole on chlorite–mica aggregates.

Despite the fact that a quartz content of larger than 25% is characteristic of granites, the rock cannot be referred to them due to the predominance of secondary quartz related to superimposed silicification. A high color index and a small amount (or, less likely, absence) of igneous quartz suggest that the initial igneous rock had a slightly different composition, with the fraction of mafic minerals being 25%, and 60–70% plagioclase, and 5–15% quartz. The igneous matrix can be referred to quartz (?) diorites, but later it underwent considerable alterations. Alteration was accompanied by the local formation of an oriented structure typical of granitic gneisses and expressed mainly in the orientation of mafic minerals.

The evolution of Balkan massif rocks includes several stages and substages. At the magmatic stage, quartz diorite crystallized from melt. Low-temperature alterations of igneous minerals, when plagioclase was saussuritized and igneous biotite was replaced by chlorite–muscovite aggregate with extraction of ore mineral and titanite, were possible both at the postmagmatic stage, typical of cooling of the massif, and at the low-temperature phase of the regional metamorphic stage. We revealed that the next stage corresponded to the prograding phase of regional metamorphism, expressed in the development of skeleton poikiloblasts of light bluish amphibole on micas and chlorite. This subalkaline amphibole is a specific feature of regional metamorphism in the Blyb metamorphic complex. Its occurrence in diorite probably indicates a change in the mineral-formation stages from postmagmatic to prograding metamorphic. The silicification phase refers to the late stage of regional metamorphic alterations that involved the intrusive massif. This stage also includes such local deformations as texturing of quartz lenses and the occurrence of kink zones.

Apart from the Balkan massif, the area where the Blyb metamorphic complex developed contains foliated granodiorites that differ from metadiorites of the Balkan massif in character of occurrence, composition, and evolutionary aspects. These granodiorites are likely confined to the series of faults in the southern part of the complex (these faults are oriented in parallel to the boundary with the Main Range zone). We denoted the largest outcrop of these rocks as the Southern intrusive body; it is located in the area of the Greater Balkanka River (Fig. 2).

SOUTHERN INTRUSIVE BODY

Rocks of the Southern intrusive body have the following mineral composition: 15% biotite, chlorite,

and muscovite; 50% plagioclase; 10% K-feldspar; and 25% quartz. The rock color index is M15.

The rock structure is irregularly spotted with distinguishable quartz lenses, feldspar clusters, and biotite–chlorite–muscovite aggregates. The rock is visibly lineated: chlorite–mica aggregates are elongated in one direction and crossed by chaotically oriented veins of sericite, chlorite, epidote, and calcite. The rock texture is medium-grained; the primary igneous minerals (which include feldspars, interstitial quartz, and biotite) make up a hypidiomorphic texture with predominant idiomorphism of feldspars with respect to quartz. Superimposed textures formed by secondary minerals—reaction (biotite replacement with chlorite and sphene), corrosion (replacement of plagioclase relics in quartz lenses), and blastocataclastic (within elongated chlorite–epidote veins) are locally observed. A higher color index and relatively small (for granite) contents of microcline and primary quartz suggest that the initial igneous rock contained 15% mafic minerals, 65% feldspars, and 20% quartz.

This rock can be referred to granodiorites that underwent subsequent low-temperature structural–metamorphic alteration.

The evolution of this rock is quite simple and includes fewer stages and phases with respect to metadiorites from the Balkan massif, because magmatic minerals and texture are better preserved, but brittle deformations and foliation are manifested more intensively. The latter features indicate the presence of oriented stresses in the solid massif. We found that the igneous stage of the evolution of the Southern intrusive body was related to crystallization of granodiorite from melt, whereas the stage of structural metamorphism (low-temperature replacement of magmatic minerals, silicification) was accompanied by internal deformations of the massif.

METAMORPHIC EVOLUTION OF INTRUSIONS AND HOST ROCKS

Below, the metamorphic evolutions in the Balkan massif, Southern intrusive body, and host rocks of the Blyb complex are compared to reveal the main stages of transformations and to correlate the manifestations of magmatic and metamorphic processes with time.

We distinguished five major stages in the evolution of rocks making up the Blyb metamorphic complex.

We found relics of a high-pressure mineral association in these rocks. In addition, eclogite blocks can be seen there [8]. Taking into consideration studies of phengites from gneisses and schists of the Blyb complex, we can assume that these rocks underwent high-pressure metamorphism, which we regard as the first stage of metamorphism.

At the second stage, the discussed rocks demonstrated signs of subsequent deep alteration under epi-

dote–amphibole facies conditions to form a ubiquitous association of light bluish amphibole with epidote.

The third stage was superimposed albitization, which involved all rocks of the Blyb metamorphic complex, but to different degrees.

The fourth and fifth stages are the final phases in the evolution of the complex: cataclasis and recrystallization followed by low-temperature retrograde metamorphism that included acidic and alkaline phases pertaining to silicification and replacement of amphibole and epidote with biotite, respectively.

The history of rock transformations in the Balkan massif and Southern intrusive body allowed us to estimate the positions of these objects in the evolution of the entire Blyb metamorphic complex. For example, quartz diorites of the Balkan massif contain no evidence of high-pressure metamorphism. Beginning from the stage of regional metamorphism, under epidote–amphibolite facies conditions, rocks of the Balkan massif and host rocks of the Blyb metamorphic complex underwent a joint evolution. Rocks of the Southern intrusive body bear no traces of the stage of amphibole poikiloblasts on chlorite, whereas it is represented in Balkan massif metadiorites and the Blyb metamorphic complex. Thus, the metamorphic evolution of the Southern intrusive body is limited to low-temperature metamorphism and silicification, hence indicating the younger age of the Southern intrusive body.

U–Pb AGE DETERMINATION FOR INTRUSIVE BODIES IN THE AREA OF THE MALAYA LABA RIVER

To determine the ages of intrusive bodies in the Blyb metamorphic complex, we dated zircons by U–Pb method. Analyses were performed on a SHRIMP-II ion microprobe at the Center for Isotope Research (Karpinsky Russian Geological Research Institute, St. Petersburg) using the standard technique [26, 36]. Zircons were sampled manually using an optical microprobe and were then placed in an epoxy matrix with 91500 [35] and Temora [15] standard zircons. The zircons were faced until about half their thickness. The internal structure of zircon grains was studied with an optical microprobe and cathode luminescence. For our analysis, we preferably selected zones with low-intensity cathode luminescence and those without visible cracks or inclusions. The surfaces of samples were coated with 99.999% gold 0.01 μm thick. Ion currents were measured by a secondary ion multiplier in the mass scanning mode. The sample material was ionized by bombardment of the analyzed sites of zircon grains by a flux of primary O_2^- . An elliptic analytical point $27 \times 20 \mu\text{m}$ in size was obtained using a 120 μm Kohler aperture. The ion current of the primary beam was from -4.4 to -4.6 nA. Secondary ions were guided to the mass spectrometer by a 10 kV accelerating poten-

tial. To validate the center of the peak ion current in each mass spectrum, we used ions with masses of 196 (Zr_2O) and 254 (UO) during analysis. Each analytical session began and ended with standard zircon measurements. Every fourth measurement was done for a Temora standard zircon.

The results were processed with SQUIDv1.12 and ISOPLOT/Exv3.22 software [27, 28], employing the decay constants proposed by R.H. Steiger and E. Jäger [32]. To introduce the correction to common lead using the model by J.S. Stacey and J.D. Kramers [31], we used the $^{204}\text{Pb}/^{206}\text{Pb}$ ratio.

The obtained dates for granitoids from the area of the Malaya Laba River allowed us to determine the time of magmatic events in the basement of the Fore Range zone. Zircons were extracted from two granitoid samples collected in the western part of the Balkan intrusive massif, exposed by the channel of Malaya Laba River (Fig. 2). The distance between sample collection points was 1 km. Zircons from sample 16-5a ($n = 10$) are euhedral (idiomorphic), possessing clear oscillatory zoning (Figs. 3b and 3c', Table 1); given the high Th/U ratios (0.45–1.27), these zircons are of magmatic origin [14, 19, 22, 29, 30]. The peculiarities of this sample are high density of the obtained dates and extremely low values of mean square weighted deviation (MSWD = 0.00084). The concordant age on this sample is 574.1 ± 6.7 Ma. The sample 16-4a ($n = 8$) is also typical of euhedral zircons with fine oscillatory zoning (Figs. 3c, 3c', Table 2). These Th/U values (0.38–1.01) are also characteristic of igneous zircons. The concordant age of this sample is 567.9 ± 6.9 Ma (MSWD = 0.049).

The ages of both samples correspond to the Late Vendian and support the earlier date obtained in the northern margin of the Balkan massif (sample 124-1), whose concordant age was 549 ± 7.4 Ma (Figs. 3a, 3a'; Table 3) [4]. Three dates for samples 124-1, 16-4a, and 16-5a are almost identical in both age and morphology of zircons. Taking into account the spatial locations of the samples, we revealed large outcrops of Late Vendian rocks in the Malaya Laba River Basin.

Two kilometers to the south of the sampling site of the Balkan intrusive massif, in the granodiorite outcrop zone of the Southern intrusive body, we also collected sample 16-6a for dating (Fig. 2). The concordant age obtained on euhedral zircons ($n = 10$) with clear oscillatory zoning was 319 ± 3.8 Ma (MSWD = 0.14) (Figs. 3d, 3d'; Table 4); the Th/U ratios (0.31–0.51) indicate magmatic genesis of zircons. This age value corresponds to the end of Serpukhovian stage, Early Carboniferous.

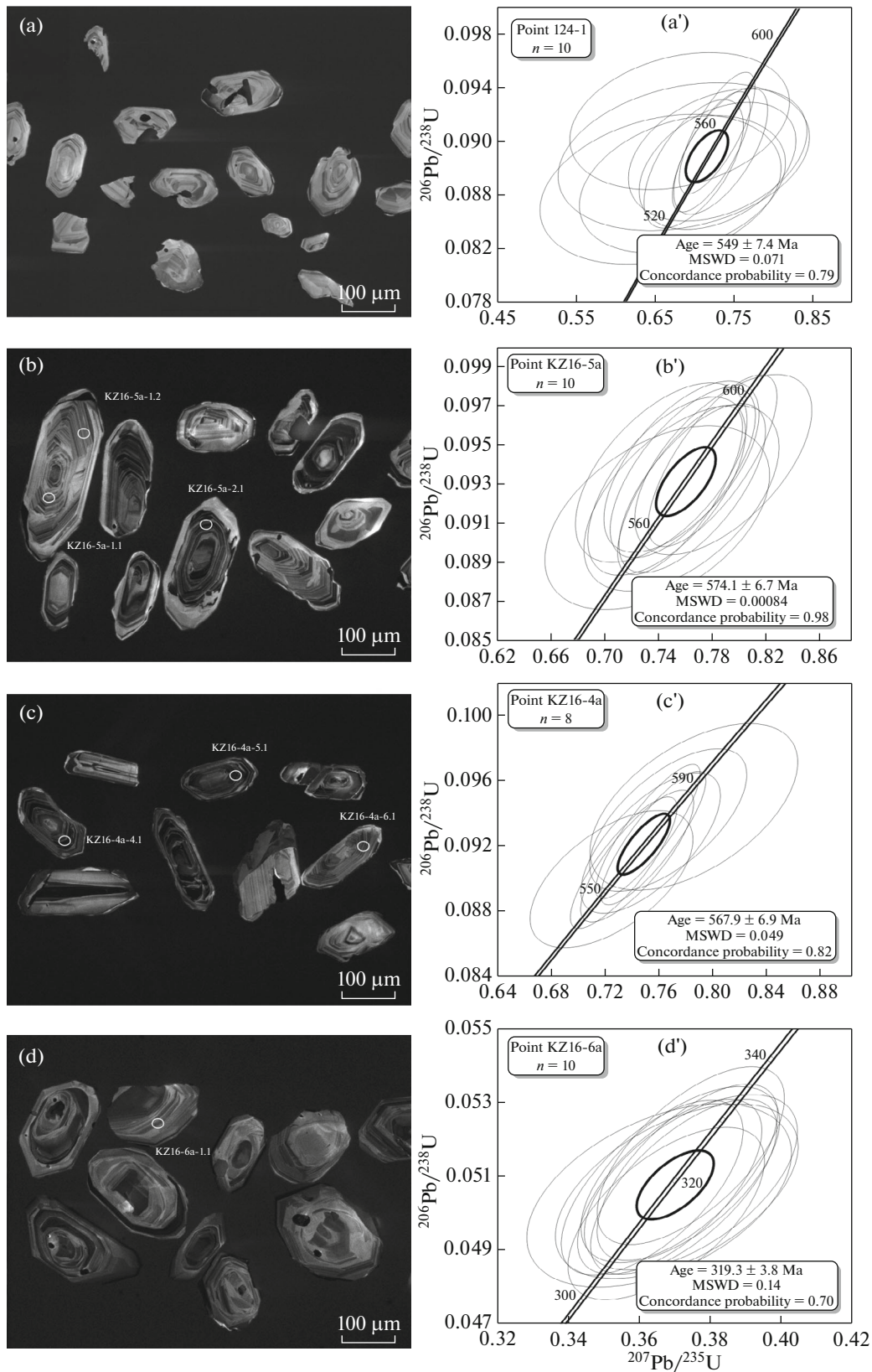


Fig. 3. Cathode luminescent images of studied zircons and respective concordia plots: (a) and (a'), Balkan massif (northern contact zone, Koptseva gully, point 124-1); (b) and (b'), Balkan massif (Sukhaya gully area, point KZ16-5a); (c) and (c'), Balkan massif (southern part, Bol'shaya Balkanka River, point KZ16-4a); (d) and (d'), Southern intrusive body of granodiorites (point KZ16-6a). Ellipses of measurements errors have 2 σ confidence intervals.

Table 1. Results of U–Pb isotope dating and calculated ages for zircons from quartz metadiorites of Balkan massif (point KZ16-5a)

Point	$^{206}\text{Pb}_c$, %	U, Ma^{-1}	Th, Ma^{-1}	$^{232}\text{Th}/^{238}\text{U}$	$^{206}\text{Pb}^*$, Ma^{-1}	$^{206}\text{Pb}/^{238}\text{U}$ age ¹ , Ma	Total $^{238}\text{U}/^{206}\text{Pb}$	Total $^{207}\text{Pb}/^{206}\text{Pb}$	$^{238}\text{U}/^{206}\text{Pb}^*$	$^{207}\text{Pb}^*/^{206}\text{Pb}^*$	$^{207}\text{Pb}^*/^{235}\text{U}^1$	$^{206}\text{Pb}^*/^{238}\text{U}^1$	ρ
KZ16-5a-1.1	0.15	2041	1532	0.78	163.0	572 ± 11	10.75 ± 2.0%	0.0594 ± 2.2%	10.8 ± 2.0%	0.0582 ± 2.6%	0.746 ± 3.2%	0.0929 ± 2.0%	0.604
KZ16-5a-1.2	0.00	1297	657	0.52	105.0	579 ± 11	10.64 ± 2.0%	0.0608 ± 2.7%	10.6 ± 2.0%	0.0608 ± 2.7%	0.788 ± 3.4%	0.0940 ± 2.0%	0.602
KZ16-5a-2.1	0.05	3872	2775	0.74	313.0	580 ± 10	10.61 ± 1.9%	0.0605 ± 1.6%	10.6 ± 1.9%	0.0601 ± 1.6%	0.780 ± 2.5%	0.0942 ± 1.9%	0.752
KZ16-5a-3.1	0.00	2165	2488	1.19	174.0	577 ± 11	10.68 ± 1.9%	0.0587 ± 2.1%	10.7 ± 1.9%	0.0587 ± 2.1%	0.758 ± 2.9%	0.0936 ± 1.9%	0.670
KZ16-5a-4.1	0.14	1504	655	0.45	121.0	577 ± 11	10.67 ± 2.0%	0.0586 ± 2.5%	10.7 ± 2.0%	0.0575 ± 2.8%	0.742 ± 3.5%	0.0936 ± 2.0%	0.578
KZ16-5a-5.1	0.28	1017	456	0.46	80.0	563 ± 11	10.92 ± 2.1%	0.0610 ± 3.1%	11.0 ± 2.1%	0.0587 ± 4.1%	0.739 ± 4.6%	0.0913 ± 2.1%	0.462
KZ16-5a-6.1	0.00	2139	1515	0.73	170.0	572 ± 11	10.78 ± 1.9%	0.0598 ± 2.1%	10.8 ± 1.9%	0.0598 ± 2.1%	0.765 ± 2.9%	0.0928 ± 1.9%	0.673
KZ16-5a-7.1	0.20	2987	2337	0.81	241.0	578 ± 10	10.63 ± 1.9%	0.0602 ± 1.8%	10.7 ± 1.9%	0.0585 ± 2.4%	0.757 ± 3.1%	0.0939 ± 1.9%	0.614
KZ16-5a-8.1	0.00	980	464	0.49	77.7	569 ± 12	10.83 ± 2.1%	0.0594 ± 3.3%	10.8 ± 2.1%	0.0594 ± 3.3%	0.757 ± 3.9%	0.0923 ± 2.1%	0.544
KZ16-5a-9.1	0.00	3230	3974	1.27	257.0	571 ± 10	10.79 ± 1.9%	0.0592 ± 1.7%	10.8 ± 1.9%	0.0592 ± 1.7%	0.756 ± 2.5%	0.0927 ± 1.9%	0.739

ρ is error correlation. Errors are given for 1 σ confidence interval. Pb_c and Pb^* correspond to total contents of all common and radiogenic lead, respectively. Error when calibrating by standards is 0.57% (not accounted for in shown error values). Superscript ¹ means that total lead content was corrected by ^{204}Pb .

Table 2. Results of U–Pb isotope dating and calculated ages for zircons from quartz metadiorites of Balkan massif (point KZ16-4a)

Point	$^{206}\text{Pb}_c$, %	U, Ma^{-1}	Th, Ma^{-1}	$^{232}\text{Th}/^{238}\text{U}$	$^{206}\text{Pb}^*$, Ma^{-1}	$^{206}\text{Pb}/^{238}\text{U}$ age ¹ , Ma	Total $^{238}\text{U}/^{206}\text{Pb}$	Total $^{207}\text{Pb}/^{206}\text{Pb}$	$^{238}\text{U}/^{206}\text{Pb}^* \pm 1$	$^{207}\text{Pb}^*/^{206}\text{Pb}^* \pm 1$	$^{207}\text{Pb}^*/^{235}\text{U} \pm 1$	$^{206}\text{Pb}^*/^{238}\text{U} \pm 1$	ρ
KZ16-4a-7.1	0.91	1829	978	0.55	134.0	525.0 ± 10.0	$11.69 \pm 2.0\%$	$0.0731 \pm 5.9\%$	$11.80 \pm 2.0\%$	$0.0658 \pm 7.7\%$	$0.769 \pm 8.0\%$	$0.0848 \pm 2.0\%$	0.256
KZ16-4a-9.1	0.11	1839	961	0.54	135.0	529.0 ± 10.0	$11.68 \pm 2.0\%$	$0.0590 \pm 2.4\%$	$11.69 \pm 2.0\%$	$0.0580 \pm 2.6\%$	$0.684 \pm 3.3\%$	$0.0855 \pm 2.0\%$	0.618
KZ16-4a-2.1	0.17	2206	1472	0.69	171.0	556.0 ± 10.0	$11.09 \pm 1.9\%$	$0.0598 \pm 2.1\%$	$11.11 \pm 1.9\%$	$0.0584 \pm 2.7\%$	$0.725 \pm 3.4\%$	$0.0900 \pm 1.9\%$	0.577
KZ16-4a-10.1	0.00	6889	4372	0.66	539.0	561.7 ± 9.8	$10.98 \pm 1.8\%$	$0.0585 \pm 1.2\%$	$10.98 \pm 1.8\%$	$0.0585 \pm 1.2\%$	$0.734 \pm 2.2\%$	$0.0910 \pm 1.8\%$	0.835
KZ16-4a-4.1	0.00	5438	3554	0.68	427.0	563.7 ± 9.9	$10.94 \pm 1.8\%$	$0.0591 \pm 1.4\%$	$10.94 \pm 1.8\%$	$0.0591 \pm 1.4\%$	$0.744 \pm 2.3\%$	$0.0914 \pm 1.8\%$	0.806
KZ16-4a-6.1	0.08	2620	1699	0.67	208.0	569.0 ± 10.0	$10.83 \pm 1.9\%$	$0.0599 \pm 1.9\%$	$10.84 \pm 1.9\%$	$0.0593 \pm 2.1\%$	$0.754 \pm 2.8\%$	$0.0922 \pm 1.9\%$	0.681
KZ16-4a-5.1	0.02	8413	5163	0.63	669.0	570.3 ± 9.9	$10.81 \pm 1.8\%$	$0.0595 \pm 1.1\%$	$10.81 \pm 1.8\%$	$0.0593 \pm 1.1\%$	$0.756 \pm 2.1\%$	$0.0925 \pm 1.8\%$	0.854
KZ16-4a-3.1	0.06	10474	10282	1.01	837.0	572.7 ± 10.0	$10.76 \pm 1.8\%$	$0.0591 \pm 1.0\%$	$10.76 \pm 1.8\%$	$0.0587 \pm 1.1\%$	$0.752 \pm 2.1\%$	$0.0929 \pm 1.8\%$	0.860
KZ16-4a-1.1	0.00	2387	1645	0.71	192.0	577.0 ± 11.0	$10.69 \pm 1.9\%$	$0.0595 \pm 2.4\%$	$10.69 \pm 1.9\%$	$0.0595 \pm 2.4\%$	$0.767 \pm 3.1\%$	$0.0936 \pm 1.9\%$	0.634
KZ16-4a-8.1	0.00	829	305	0.38	67.3	581.0 ± 12.0	$10.59 \pm 2.2\%$	$0.0604 \pm 3.4\%$	$10.59 \pm 2.2\%$	$0.0604 \pm 3.4\%$	$0.786 \pm 4.0\%$	$0.0944 \pm 2.2\%$	0.537

ρ is error correlation. Errors are given for 1 σ confidence interval. Pb_c and Pb^* correspond to total contents of all common and radiogenic lead, respectively. Error when calibrating by standards is 0.57% (not accounted for in shown error values). Superscript ¹ means that total lead content was corrected by ^{204}Pb .

Table 3. Results of U–Pb isotope dating and calculated ages for zircons from quartz metadiorites of Balkan massif (point 124-1)

Point	$^{206}\text{Pb}_c$, %	U, Ma^{-1}	Th, Ma^{-1}	$^{232}\text{Th}/^{238}\text{U}$	$^{206}\text{Pb}^*$, Ma^{-1}	$^{206}\text{Pb}/^{238}\text{U}$ age ¹ , Ma	Dis, %	$^{207}\text{Pb}^*/^{235}\text{U}^1$	$^{206}\text{Pb}^*/^{238}\text{U}^1$, %	ρ
124-1_1.1	0.00	87	83	0.99	6.60	546 ± 12	–7	0.699 ± 3.7	0.0884 ± 2.2	0.603
124-1_2.1	0.09	304	668	2.27	23.30	551 ± 11	0	0.721 ± 2.8	0.0893 ± 2.0	0.734
124-1_3.1	0.84	48	28	0.61	3.58	535 ± 14	–22	0.657 ± 9.5	0.0865 ± 2.6	0.278
124-1_4.1	0.42	76	61	0.83	5.78	545 ± 11	10	0.729 ± 5.6	0.0882 ± 2.2	0.395
124-1_5.1	0.80	56	25	0.47	4.31	549 ± 13	–18	0.686 ± 9.5	0.0889 ± 2.5	0.267
124-1_6.1	1.06	78	47	0.62	6.20	565 ± 12	–35	0.681 ± 8.3	0.0916 ± 2.3	0.273
124-1_7.1	0.69	52	23	0.47	3.88	537 ± 12	–7	0.685 ± 7.8	0.0868 ± 2.4	0.310
124-1_8.1	0.00	112	83	0.77	8.58	551 ± 11	6	0.733 ± 3.3	0.0893 ± 2.2	0.651
124-1_9.1	0.60	76	39	0.53	5.82	550 ± 12	6	0.729 ± 6.3	0.0890 ± 2.3	0.357
124-1_10.1	0.09	304	928	3.16	23.70	559 ± 11	–3	0.728 ± 2.7	0.0907 ± 2.0	0.759

Dis is discordance; ρ , errors correlation. Errors are given for 1σ confidence interval. Pb_c and Pb^* correspond to total contents of all common and radiogenic lead, respectively. Error when calibrating by standards is 0.55% (not accounted for in shown error values). Superscript ¹ means that total lead content was corrected by ^{204}Pb .

ANISOTROPY OF MAGNETIC SUSCEPTIBILITY IN INTRUSIVE BODIES OF THE AREA OF THE MALAYA LABA RIVER

To reconstruct the conditions of emplacement and evolution of the Balkan massif and Southern granitic intrusive body, we measured the anisotropy of magnetic susceptibility. Magnetic fabric studies are widely used to reconstruct magmatic and structural evolution of granite massifs; they are especially effective if macroscopic orientation is weakly expressed [16, 17, 21, 25, 34]. We examined 14 sites in the Balkan massif, the Southern intrusive body, and host metamorphic rocks of the Blyb complex. At each site, 10–20 oriented samples were collected.

The anisotropy of magnetic susceptibility (AMS) was measured with a Kappabridge MFK1-FA (AGICO, Czech Republic) at the Laboratory for Main Geomagnetic Field and Petromagnetism (Schmidt Institute of Physics of the Earth, Russian Academy of Sciences, Moscow) and at the petromagnetic laboratory, Department of Geology, Moscow State University. The measurements were processed in Anisoft 4.2 software [18] using Jelinek statistics [23].

The measurement results are presented in the form of a triaxial AMS ellipsoid (Fig. 4). The value of bulk magnetic susceptibility in granitoid samples from the Balkan massif varied from 1.4×10^{-4} to 2.5×10^{-3} SI units, while that for the Southern intrusive body was from 1.5×10^{-4} to 1.4×10^{-3} SI units; hence, the studied rocks are intermediate between magnetitic and ilmenitic granites in terms of this parameter [20, 34]. This indicates a possible considerable contribution from both ferromagnetic and paramagnetic minerals to magnetic anisotropy. For the host metamorphic rocks, the value of the overall magnetic susceptibility varied in the range of $7.3\text{--}8.2 \times 10^{-4}$ SI units.

The values of parameter P_j , showing the corrected degree of anisotropy [24], are minimum for granodiorites of the Southern intrusive body (1.01–1.06), and these values are typical of weakly metamorphosed igneous rocks that did not undergo significant tectonic reworking [34]. For the Balkan massif, this parameter is 1.03–1.06 on average in the central part (Fig. 5, sites 22–24), 1.04–1.07 in the northern contact (sites 25 and 26), and 1.06–1.10 in the eastern contact (sites 13–15 and 18); for host gneisses and schists of the Blyb complex, it is 1.1–1.2. Parameter T , characterizing the ellipsoid shape of AMS, is positive on average at the majority of sampling sites and corresponds to an oblate ellipsoid (Table 5). However, there is no apparent dependence between the P_j and T values.

At four sites in granitoids of the Balkan massif (its eastern contact zone), the AMS ellipsoid appeared to be of the so-called normal type, with the minimum ellipsoid axis K_3 being oriented perpendicular to the mineral foliation and the maximum (K_1) and intermediate (K_2) axes being in the plane of the foliation (Fig. 4b). For example, at sites 13–15, the minimum axis changes its orientation approaching the contact: from gentle westward dips to steep northwestward ones and then to southwestward, rotating with the pole of the macroscopic foliation. In metamorphic rocks of the Blyb complex, near the contact of the Balkan massif, the minimum K_3 axis is also normal to the gneissic structure but has an abruptly different orientation (Fig. 4a; Table 5). These differences between closely located sampling points corresponding to the Balkan massif and its surrounding rocks indicate the absence of significant tectonic stresses, which could have simultaneously affected the magnetic textures of granitoids and host rocks; as well, there was no contact effect of the massif on metamorphic rocks of the

Table 4. Results of U–Pb isotope dating and calculated ages for zircons from granodiorites of Southern intrusive body (point KZ16-6a)

Point	$^{206}\text{Pb}_c$, %	U, Ma^{-1}	Th, Ma^{-1}	$^{232}\text{Th}/$ ^{238}U	$^{206}\text{Pb}^*$, Ma^{-1}	$^{206}\text{Pb}/^{238}\text{U}$ age ¹ , Ma	Total $^{238}\text{U}/^{206}\text{Pb}$	Total $^{207}\text{Pb}/^{206}\text{Pb}$	$^{238}\text{U}/^{206}\text{Pb}^*$	$^{207}\text{Pb}^*/^{206}\text{Pb}^*$	$^{207}\text{Pb}^*/^{235}\text{U}^1$	$^{206}\text{Pb}^*/^{238}\text{U}^1$	ρ
KZ16-6a-1.1	0.00	2691	934	0.36	117	317.5 ± 6.1	$19.81 \pm 2.0\%$	$0.0525 \pm 3.8\%$	$19.81 \pm 2.0\%$	$0.0525 \pm 3.8\%$	$0.366 \pm 4.2\%$	$0.0505 \pm 2.0\%$	0.460
KZ16-6a-2.1	0.00	3985	1213	0.31	174	318.8 ± 5.9	$19.72 \pm 1.9\%$	$0.0520 \pm 2.2\%$	$19.72 \pm 1.9\%$	$0.0520 \pm 2.2\%$	$0.364 \pm 2.9\%$	$0.0507 \pm 1.9\%$	0.647
KZ16-6a-3.1	0.00	4382	1815	0.43	191	319.0 ± 6.0	$19.71 \pm 1.9\%$	$0.0533 \pm 2.1\%$	$19.71 \pm 1.9\%$	$0.0533 \pm 2.1\%$	$0.373 \pm 2.9\%$	$0.0507 \pm 1.9\%$	0.674
KZ16-6a-4.1	0.12	4454	1585	0.37	192	314.5 ± 5.8	$19.98 \pm 1.9\%$	$0.0544 \pm 2.1\%$	$20.00 \pm 1.9\%$	$0.0534 \pm 2.4\%$	$0.368 \pm 3.1\%$	$0.0500 \pm 1.9\%$	0.614
KZ16-6a-5.1	0.14	3598	1697	0.49	157	319.7 ± 5.9	$19.64 \pm 1.9\%$	$0.0546 \pm 2.3\%$	$19.67 \pm 1.9\%$	$0.0535 \pm 2.7\%$	$0.375 \pm 3.3\%$	$0.0508 \pm 1.9\%$	0.581
KZ16-6a-6.1	0.00	3922	1325	0.35	174	324.1 ± 6.0	$19.39 \pm 1.9\%$	$0.0528 \pm 2.2\%$	$19.39 \pm 1.9\%$	$0.0528 \pm 2.2\%$	$0.375 \pm 2.9\%$	$0.0516 \pm 1.9\%$	0.648
KZ16-6a-7.1	0.00	4774	2029	0.44	210	321.3 ± 5.9	$19.57 \pm 1.9\%$	$0.0530 \pm 2.1\%$	$19.57 \pm 1.9\%$	$0.0530 \pm 2.1\%$	$0.374 \pm 2.8\%$	$0.0511 \pm 1.9\%$	0.670
KZ16-6a-8.1	0.00	3961	1465	0.38	173	318.9 ± 5.9	$19.72 \pm 1.9\%$	$0.0528 \pm 2.3\%$	$19.72 \pm 1.9\%$	$0.0528 \pm 2.3\%$	$0.369 \pm 2.9\%$	$0.0507 \pm 1.9\%$	0.642
KZ16-6a-9.1	0.16	4665	2323	0.51	205	321.0 ± 5.9	$19.56 \pm 1.9\%$	$0.0541 \pm 2.0\%$	$19.59 \pm 1.9\%$	$0.0529 \pm 2.5\%$	$0.372 \pm 3.1\%$	$0.0511 \pm 1.9\%$	0.603
KZ16-6a-10.1	0.19	2755	816	0.31	120	318.2 ± 6.0	$19.72 \pm 1.9\%$	$0.0548 \pm 2.6\%$	$19.76 \pm 1.9\%$	$0.0532 \pm 3.2\%$	$0.371 \pm 3.8\%$	$0.0506 \pm 1.9\%$	0.515

ρ is error correlation. Errors are given for 1 σ confidence interval. Pb_c and Pb^* correspond to total contents of all common and radiogenic lead, respectively. Error when calibrating on standards is 0.57% (not accounted for in shown error values). Superscript ¹ means that total lead content was corrected by ^{204}Pb .

Fig. 4. Examples of AMS measurement results for studied objects: (a) site 16, metamorphic rocks of Blyb complex; (b) site 13, Balkan massif; (c) site 21, Southern intrusive body. Stereographic equal-area projection, lower hemisphere. (1) Maximum axis of AMS ellipsoid; (2) intermediate axis; (3) minimum axis; (4) orientation of macroscopic foliation plane; (5) poles to macroscopic foliation.

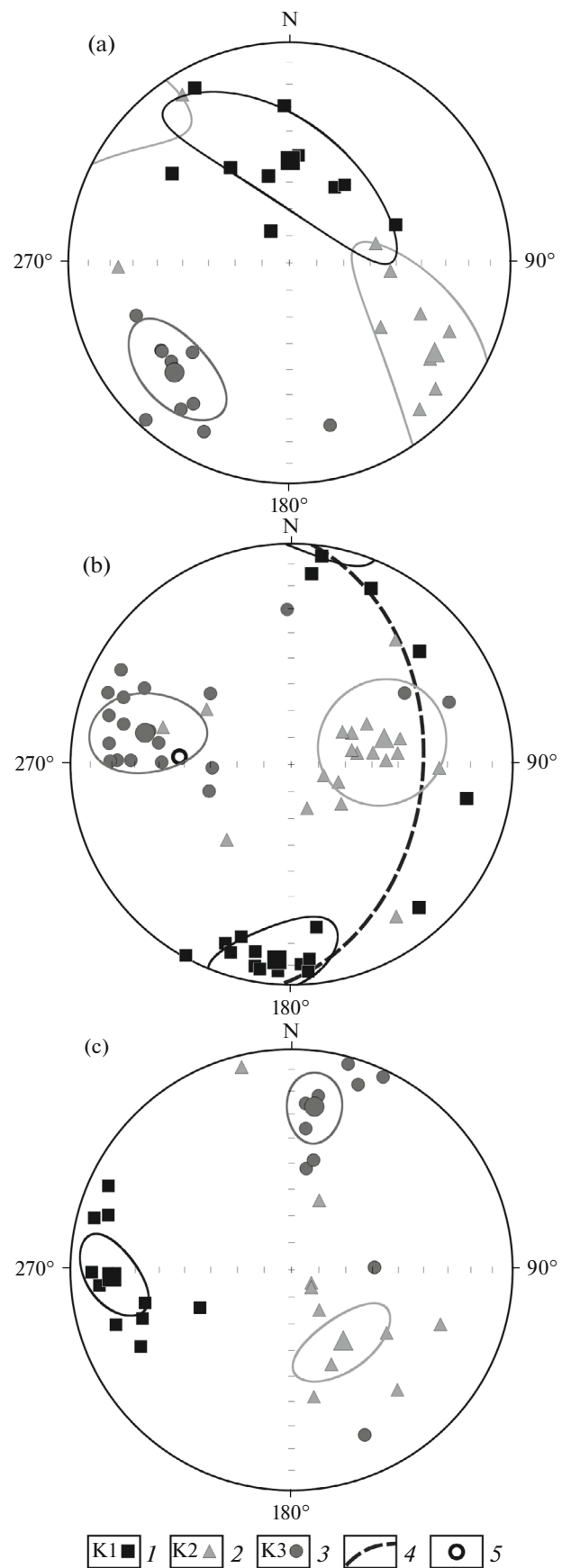
Armovka Formation of the Blyb complex sampled at site 16 (Fig. 5). At the same time, this result may indicate tectonic coupling of Balkan massif granitoids and spatially associated rocks of the Armovka Formation.

In the central and northern parts of the Balkan massif, there is usually no regular macroscopic foliation (Table 4). The directions of the axes of AMS ellipsoid significantly differ between sites. Since the degree of anisotropy at these sites is relatively low compared to the eastern contact of the massif, orientation of the minimum K3 axis is seemingly determined by the positions of intrusive contacts and local faults (Fig. 5).

At all three sites corresponding to granodiorites of the Southern intrusive body, the magnetic foliation occurs at a steep angle and extends in the northwestern direction; near the northern contact of the intrusive body (site 21), the minimum K3 axis dips gently northward, whereas in the southern part of the intrusive body (sites 17 and 20), the axis dips southward. Since granitoids of this massif are characterized by a low degree of anisotropy and a predominantly oblate shape of the ellipsoid, we interpret the magnetic texture in samples from the Southern intrusive body as primary magmatic, related to contact stress during melt cooling after emplacement. In this case, the orientation of the minimum K3 axis is perpendicular to the contact of the massif, and the magnetic foliation is parallel to the contact plane. Hence, the shape of the Southern intrusive body can be described as a NW-elongated linear swell extending along a regional fault (Fig. 4c), in parallel to the southern boundary of the Fore Range zone.

DISCUSSION

As a result of our studies, large outcrops of Precambrian rocks have been revealed within the limits of the Blyb metamorphic complex. The most ancient among the studied rocks of the Fore Range pertain to the Late Vendian and make up a Balkan massif of quartz metadiorites which is at least 33 km² in total area. Near the northwestern limit of the Balkan massif, a thick (at least 500 m) member of migmatite-like rocks occurs; it is represented by alternation of amphibolites, garnet amphibolites, and leucocratic veins (Fig. 2), which can be considered as host rocks of the Balkan massif because the latter contain fragments of the former as xenoliths. The ancient rocks of the Balkan Formation and metadiorite massif are overlain by leucocratic garnet–mica gneisses, quartz–mica gneisses, and garnet–kyanite gneisses that are common on both sides of Malaya Laba River Valley and are also exposed in



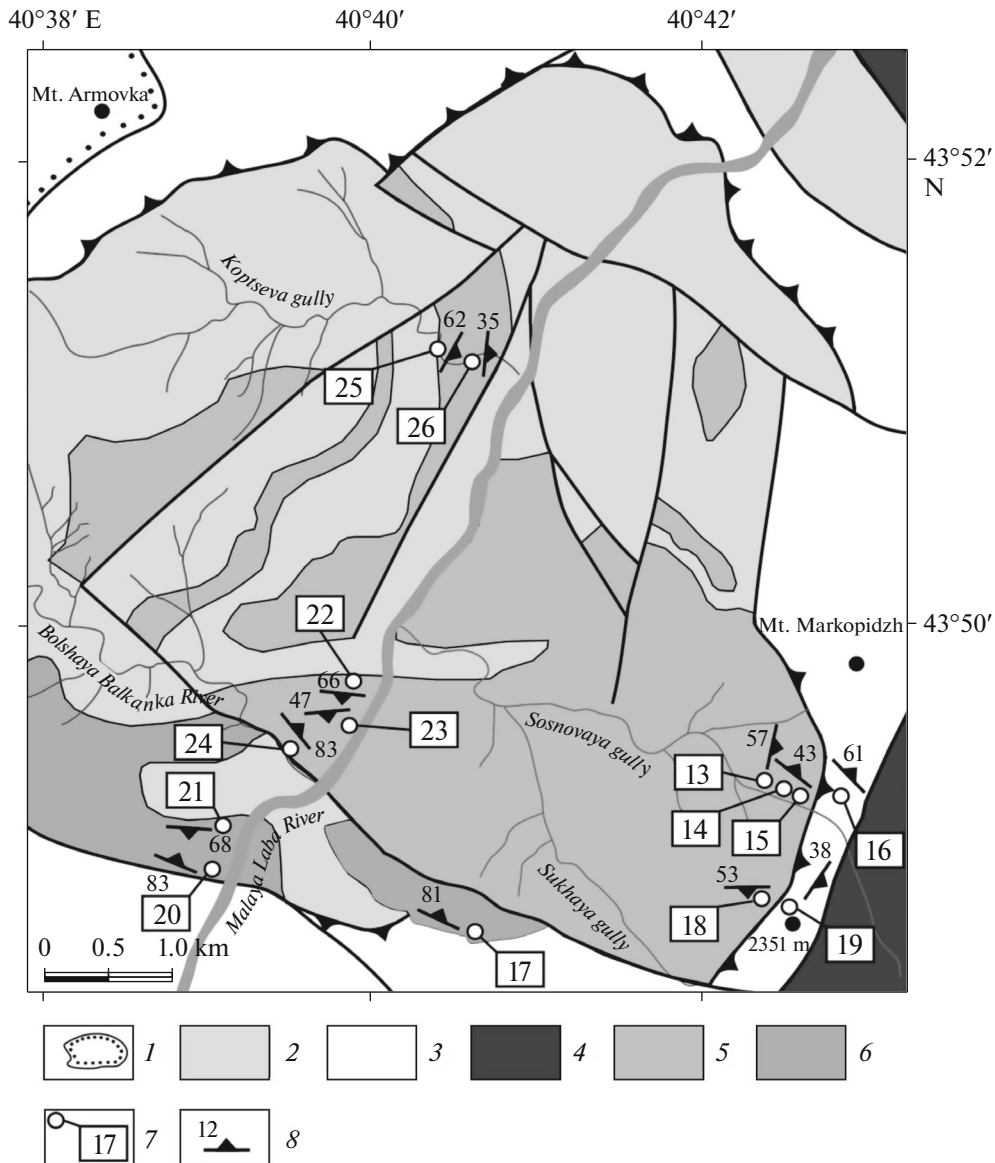


Fig. 5. Structural scheme of Blyb metamorphic complex in area of Balkan massif with orientations of magnetic foliation at studied sites (with data from [5]). (1) Triassic deposits; (2) Balkan Formation; (3) Armovka metamorphic rocks; (4) serpentinite bodies; (5) Balkan massif; (6) granodiorite intrusions; (7) numbers and locations of sites of AMS measurements; (8) magnetic foliation.

the central and southern parts of the Blyb metamorphic complex within the area of Bol'shaya Laba River (Armovka Formation) [5]. These overlying rocks are associated with large serpentinite bodies and blocks of eclogites and apoeclomite garnet amphibolites. The age of overlying rocks has been determined as Middle Paleozoic [6, 33]. For example, paragneisses of the Greater Blyb stream valley, which are located in the structurally upper part of the section of the Blyb metamorphic complex (lower parts of the complex are exposed to the south), yielded an age of 361.4 ± 3 Ma with laser ablation (LA-ICP-MS) on 25 grains.

Rocks of the Balkan massif metamorphosed under epidote–amphibolite facies conditions. The overlying

rocks demonstrate features of high-pressure metamorphism, supported by phengite monomineral barometry [9], eclogites that appear here, and findings of minerals from a high-pressure association in the form of inclusions in sulfides [4]. Thus, rocks of the Balkan massif and overlying gneisses formed in different periods, under different P – T conditions and were later coupled. The contact between Proterozoic and Middle Paleozoic rocks within the Blyb metamorphic complex is tectonic. In the area of an unnamed mountain with an absolute height of 2351 m (Fig. 2), abrupt changes in composition, degree of foliation, and orientations of gneissic structures are observed between rocks of the Balkan massif and overlying garnet–mica

Table 5. Results of AMS measurements

Site	Object	N	K, SI units	Pj	T	K1			K2			K3			Macroscopic foliation	
						D, deg	I, deg	Ci, deg	D, deg	I, deg	Ci, deg	D, deg	I, deg	Ci, deg	Az, deg	Dip, deg
13	B	19	7.26×10^{-4}	1.075	0.161	184.2	12.3	23.0/12.8	76.5	54.4	25.3/21.9	282.3	32.9	24.5/13.0	93	42
14	B	15	2.38×10^{-3}	1.073	0.033	177.9	19.5	28.2/22.1	79.5	22.4	33.9/26.3	305.1	59.6	33.2/22.7	136	28
15	B	12	1.57×10^{-3}	1.104	0.103	349.1	32.0	13.6/9.1	96.8	26.0	19.5/11.5	217.8	46.5	19.0/8.1	24	50
16	A	10	7.36×10^{-4}	1.135	0.464	0.5	51.7	51.7/15.6	122.8	22.9	51.9/16.1	226.3	28.8	19.7/14.3	46	74
17	S	17	1.32×10^{-3}	1.061	0.357	102.8	52.5	55.4/15.4	301.8	35.9	55.3/14.8	205.0	9.2	18.7/11.2	—	—
18	B	16	7.49×10^{-4}	1.062	-0.249	233.1	38.3	37.7/23.2	115.4	30.5	39.4/29.4	359.3	36.7	32.6/23.2	181	53
19	A	14	8.13×10^{-4}	1.100	0.054	204.7	7.6	24.0/11.9	108.9	37.3	39.9/18.9	304.4	51.7	40.5/15.9	286	45
20	S	14	1.71×10^{-4}	1.032	0.329	110.1	22.1	39.5/17.0	308.1	66.9	39.5/19.0	202.7	6.5	19.4/16.7	—	—
21	S	14	1.58×10^{-4}	1.014	0.008	268.1	13.6	20.3/8.9	149.0	63.5	25.1/20.1	3.8	22.2	24.9/9.0	—	—
22	B	20	4.42×10^{-3}	1.052	0.222	104.5	18.3	58.8/15.9	227.9	59.0	58.9/14.2	6.0	24.1	18.4/17.6	—	—
23	B	11	1.07×10^{-3}	1.027	0.225	100.2	16.1	38.1/16.8	205.8	42.9	38.1/18.5	354.8	42.7	19.3/16.8	—	—
24	B	14	2.26×10^{-3}	1.050	0.062	137.6	26.8	9.5/7.9	334.5	62.1	17.2/9.4	231.2	7.0	17.2/8.0	—	—
25	B	20	2.81×10^{-4}	1.045	0.474	33.5	8.2	22.3/12.4	138.2	60.3	30.7/16.4	299.1	28.3	28.8/15.5	—	—
26	B	14	1.48×10^{-4}	1.064	0.328	177.4	6.2	72.9/17.8	83.1	34.3	72.9/26.4	276.3	55.0	26.7/18.5	70	30

Objects: B, Balkan massif; S, southern intrusive body; A, Armovka Formation of metamorphic rocks. K means bulk magnetic susceptibility; N, number of samples; Pj, corrected degree of anisotropy; T, parameter of AMS ellipsoid shape. K1 stands for maximum axis of ellipsoid; K2, intermediate axis; K3, minimum axis; D, declination; I, inclination; Ci, confidence ellipse ratio. For K, Pj, T, D, and I, mean values on sites are provided. Az is dip azimuth of macroscopic foliation; Dip, dip angle of macroscopic foliation.

gneisses. In the area of the southwestern slope of Mt. Markopidzh, in the contact zone, a thick (more than 200 m) member of blastomylonites occurs on metadiorites of the Balkan massif. AMS studies also show the difference between orientations of the stress fields for the Balkan massif of the Proterozoic and its overlying rocks (Fig. 5).

CONCLUSIONS

(1) Within the Blyb metamorphic complex, two magmatic events corresponding to different stages of its evolution have been distinguished. The first event occurred during the Baikalian orogeny and corresponded to the intrusion of a large massif of quartz diorites into rocks of the Balkan Formation. The second event occurred during the Herzynian orogeny, at the boundary between the Early and Middle Carboniferous. Intruded granodiorites are located in the southwestern part of the Blyb complex, at its boundary with the Main Range zone, supposedly along faults.

(2) Proterozoic rocks in the Malaya Laba River Basin are exposed in a tectonic window, and overlying Middle Paleozoic rocks occur as a thrust sheet (nappe).

(3) The distinguished structural elements of the Blyb metamorphic complex are as follows: the Late Vendian basement composed of the Balkan Formation, intruded by the Balkan massif of quartz diorites, and the Armovka nappe of the Middle Paleozoic.

ACKNOWLEDGMENTS

The research was carried out under the State funding for the Schmidt Institute of Physics of the Earth RAS and supported by the Russian Foundation for Basic Research (project nos. 16-35-00571, 16-05-01012, and 17-05-01121) and by the Government of the Russian Federation (grant no. 14.Z50.31.0017).

REFERENCES

1. G. D. Afanas'ev, *Granitoids of Ancient Intrusive Complexes of Northwest Caucasus*, Vol. 69 of *Tr. Inst. Geol. Nauk* (Akad. Nauk SSSR, Moscow, 1950) [in Russian].
2. G. I. Baranov, G. L. Donchenko, and V. F. Sidorenko, "New data on the structure of the ancient basement of Middle Paleozoic synclinorium of the Peredovoy Range, Northwest Caucasus," in *Papers on Geology and Mineral Resources of North Caucasus* (Stavropol. Kn. Izd., Stavropol, 1972), pp. 35–43.
3. I. P. Gamkrelidze and D. M. Shengeliya, *Precambrian–Paleozoic Regional Metamorphism, Granitoid Magmatism, and Geodynamics of Caucasus* (Nauchnyi mir, Moscow, 2005) [in Russian].
4. V. A. Kamzolkin, Extended Abstract of Candidate's Dissertation in Geology and Mineralogy (Inst. Fiz. Zemli Ross. Akad. Nauk, Moscow, 2013).
5. V. A. Lavrishchev, N. I. Prutskii, V. M. Semenov, et al., *State Geological Map of Russian Federation, Scale 1 : 200000. Sheet K–37–V (Krasnaya Polyana). Explanatory Note*, 2nd ed. (VSEGEI, St. Petersburg, 2000) [in Russian].

6. Yu. G. Leonov, *Greater Caucasus in the Alpine Epoch* (GEOS, Moscow, 2007) [in Russian].
7. V. L. Omel'chenko, "Position of the Blyb complex in the pre-Mesozoic crustal structure of the Front Range Zone in the Northern Caucasus," *Geotectonics* **41**, 306–314 (2007).
8. A. L. Perchuk, "Metamorphism of kyanite eclogites from the Krasnaya Skala area (Peredovoy Range, Greater Caucasus)," *Petrologiya* **1** (1), 98–109 (1993).
9. A. L. Perchuk, Extended Abstract of Doctoral Dissertation in Geology and Mineralogy (Inst. Geol. Mineral. Ross. Akad. Nauk, Moscow, 2003).
10. Yu. Ya. Potapenko, *Stratigraphy and Structure of Pre-Devonian Complexes in the North Caucasus* (KIMS, Tbilisi, 1982) [in Russian].
11. A. A. Samokhin, "Structural peculiarities of the Greater Balkan Massif, North Caucasus," *Izv. Akad. Nauk SSSR*, No. 6, 81–91 (1957).
12. S. V. Chesnokov and I. S. Krasivskaya, *Variscan Geosyncline Magmatism of the Greater Caucasus* (Nauka, Moscow, 1985) [in Russian].
13. S. B. Yashchinin, *Geology, Metallogeny, and Ore-Mineral Resources of North Caucasus in the Beginning of the 21st Century* (Kavkazskaya zdravitsa, Mineral'nye Vody, 2008) [in Russian].
14. E. Belousova, W. Griffin, S. Y. O'Reilly, and N. Fisher, "Igneous zircon: Trace element composition as an indicator of source rock type," *Contrib. Mineral. Petrol.* **143**, 602–622 (2002).
15. L. P. Black, S. L. Kamo, C. M. Allen, J. N. Aleinikoff, D. W. Davis, R. J. Korsch, and C. Foudoulis, "Temora 1: A new zircon standard for Phanerozoic U–Pb geochronology," *Chem. Geol.* **200**, 155–170 (2003).
16. G. J. Borradaile and B. Henry, "Tectonic applications of magnetic susceptibility and its anisotropy," *Earth Sci. Rev.* **42**, 49–93 (1997).
17. J. L. Bouchez, "Granite is never isotropic: An introduction to AMS studies of granitic rocks," in *Granite: From Segregation of Melt to Emplacement Fabrics*, Ed. by J. L. Bouchez, D. H. W. Hutton, and W. E. Stephens (Springer, Dordrecht, 1997), pp. 95–112.
18. M. Chadima and V. Jelínek, "Anisoft 4.2. – Anisotropy data browser," *Contrib. Geophys. Geod.* **38**, 41 (2008).
19. F. Corfu, J. M. Hanchar, P. W. O. Hoskin, and P. Kinny, "Atlas of zircon textures," *Rev. Mineral. Geochem.* **53**, 469–500 (2003).
20. B. B. Ellwood and D. B. Wenner, "Correlation of magnetic susceptibility with $^{18}\text{O}/^{16}\text{O}$ data in late orogenic granites of the southern Appalachian Piedmont," *Earth Planet. Sci. Lett.* **54**, 200–202 (1981).
21. D. Gregorova, F. Hroudá, and M. Kohut, "Magnetic fabric of the granitic composite pluton Velka Fatra Mountains (Western Carpathians, Slovakia): A Variscan remnant within the Alpine edifice?," *Geodin. Acta* **22**, 57–72 (2009).
22. C. B. Grimes, J. L. Wooden, M. J. Cheadle, and B. E. John, "'Fingerprinting' tectono-magmatic prov-

- enance using trace elements in igneous zircon,” *Contrib. Mineral. Petrol.* **170** (5), 1–26 (2015).
23. V. Jelínek and V. Kropáček, “Statistical processing of anisotropy of magnetic susceptibility measures on groups of specimens,” *Stud. Geophys. Geodaet.* **22**, 50–62 (1978).
 24. V. Jelínek, “Characterization of the magnetic fabrics of rocks,” *Tectonophysics* **79**, T63–T67 (1981).
 25. A. Joly, M. Faure, G. Martelet, and Y. Chen, “Gravity inversion, AMS and geochronological investigations of syntectonic granitic plutons in the southern part of the Variscan French Massif Central,” *J. Struct. Geol.* **31**, 421–443 (2009).
 26. A. N. Larionov, V. A. Andreichev, and D. G. Gee, “The Vendian alkaline igneous suite of northern Timan: Ion microprobe U–Pb zircon ages of gabbros and syenite,” in *The Neoproterozoic Timanide Orogen of Eastern Baltica*, Vol. 30 of *Geol. Soc. London, Mem.*, Ed. by D. G. Gee and V. L. Pease (London, 2004), pp. 69–74.
 27. K. Ludwig, *SQUID 2: A User’s Manual; Berkeley Geochronol. Center Spec. Publ. No. 5* (Berkeley, Calif., 2009). http://www.bgc.org/isoplot_etc/squid/SQUID2_5Manual.pdf.
 28. K. R. Ludwig, *User’s Manual for ISOPLOT/Ex 3.75. A Geochronological Toolkit for Microsoft Excel; Berkeley Geochronol. Center Spec. Publ. No. 5* (Berkeley, Calif., 2012). http://www.bgc.org/isoplot_etc/isoplot/Isoplot3_75-4_15manual.pdf.
 29. A. Möller, P. J. O’Brien, A. Kennedy, and A. Kröner, “The use and abuse of Th–U ratios in the interpretation of zircon,” *Geophys. Res. Abstr.* **5**, Abstr. No. 12113 (2003).
 30. D. Rubatto and D. Gebauer, “Use of cathodoluminescence for U–Pb zircon dating by ion microprobe: Some examples from the Western Alps,” in *Cathodoluminescence in Geosciences*, Ed. by M. Pagel, V. Barbin, P. Blanc, and D. Ohnenstetter (Springer, Heidelberg, 2000), pp. 373–400.
 31. J. S. Stacey and J. D. Kramers, “Approximation of terrestrial lead isotope evolution by a two-stage model,” *Earth Planet. Sci. Lett.* **26**, 207–221 (1975).
 32. R. H. Steiger and E. Jäger, “Subcommission on geochronology: Convention of the use of decay constants in geo- and cosmochronology,” *Earth Planet. Sci. Lett.* **36**, 359–362 (1977).
 33. M. L. Somin, “Pre-Jurassic basement of the Greater Caucasus: Brief overview,” *Turk. J. Earth Sci.* **20**, 545–610 (2011).
 34. D. H. Tarling and F. Hrouda, *The Magnetic Anisotropy of Rocks* (Chapman and Hall, London, 1993).
 35. M. Wiedenbeck, P. Allé, F. Corfu, W. L. Griffin, M. Meier, F. Oberli, A. Von Quadt, J. C. Roddick, and W. Spiegel, “Three natural zircon standards for U–Th–Pb, Lu–Hf, trace element and REE analyses,” *Geostand. Newslett.* **19** (1), 1–23 (1995).
 36. I. S. Williams, “U–Th–Pb geochronology by ion microprobe,” in *Applications in Microanalytical Techniques to Understanding Mineralizing Processes*, Ed. by M. A. McKibben, W. C. Shanks III, and W. I. Ridley (Soc. Econ. Geol., Littleton, Color., 1998), pp. 1–35.

Reviewers: M.G. Leonov, T.N. Kheraskova

Translated by N. Astafiev